

# Rheological Properties of PDMS Filled with CaCO<sub>3</sub>: The Effect of Filler Particle Size and Concentration

Yabin Zhou,<sup>1</sup> Shifeng Wang,<sup>1</sup> Yong Zhang,<sup>1</sup> Yinxi Zhang,<sup>1</sup> Xuhua Jiang,<sup>2</sup> Dengfeng Yi<sup>2</sup>

<sup>1</sup>Research Institute of Polymer Materials, Shanghai Jiao Tong University, Shanghai 200240, China

<sup>2</sup>Shanghai Yaohua Nano-Tech, Shanghai 200002, China

Received 20 June 2005; accepted 27 December 2005

DOI 10.1002/app.24060

Published online in Wiley InterScience (www.interscience.wiley.com).

**ABSTRACT:** The effects of filler particle size and concentration on the rheological properties of hydroxyl terminated polydimethylsiloxane (HO-PDMS) filled with calcium carbonate (CaCO<sub>3</sub>) were investigated by an advanced rheometric expansion system (ARES). The Casson model was used to describe the relationship between shear stress and shear rate for steady-state measurement. Micron-CaCO<sub>3</sub> could not afford the CaCO<sub>3</sub>/HO-PDMS suspensions obvious shear thinning behavior and a yield stress high enough, whereas nano-CaCO<sub>3</sub> could provide the suspensions with remarkable shear thinning behavior and high yield stress. Incorporation of nano-CaCO<sub>3</sub> into HO-PDMS resulted in the transformation of HO-PDMS from a mainly viscous material to a mainly elastic material. With increasing nano-CaCO<sub>3</sub> content, shear thinning behavior of nano-CaCO<sub>3</sub>/HO-PDMS suspensions became more obvious. Remarkable yield stress

was observed in nano-CaCO<sub>3</sub>/HO-PDMS suspensions with high filler content, and increased with increasing nano-CaCO<sub>3</sub> content. The degree of thixotropy was quantitatively determined using a thixotropic loop method. It was found that nano-CaCO<sub>3</sub> favored more the buildup of filler network structure in the suspensions than micron-CaCO<sub>3</sub> at the same weight fraction. Furthermore, increasing nano-CaCO<sub>3</sub> content accelerated the establishment of filler network structure in the nano-CaCO<sub>3</sub>/HO-PDMS suspensions. An overshoot phenomenon was observed in the nano-CaCO<sub>3</sub>/HO-PDMS suspensions at high shear rates. © 2006 Wiley Periodicals, Inc. *J Appl Polym Sci* 101: 3395–3401, 2006

**Key words:** calcium carbonate; nano-sized; polysiloxane; rheology; shear

## INTRODUCTION

Silicone sealant is an important material widely used in construction and decoration fields. It is usually composed of hydroxyl terminated polydimethylsiloxane (HO-PDMS), filler, crosslink agent, catalyst, and so on. For all silicone sealants, filler is important and necessary. It can not only play a reinforcement role, but also provide silicone sealant with excellent rheological properties for practical application. In previous studies, silica (especially fumed silica) is often used as the filler for silicone sealant.<sup>1</sup> Compared with fumed silica, nano-CaCO<sub>3</sub> has several remarkable benefits, such as abundant raw material resource and low price. Especially after the application of nanotechnology in CaCO<sub>3</sub> production, nano-CaCO<sub>3</sub> has exhibited a similar effect as fumed silica, such as providing silicone sealants with high mechanical strength and excellent rheological properties. To our knowledge, few publications have concerned with the effect of nano-CaCO<sub>3</sub> on rheological properties of silicone sealants.<sup>2</sup>

In fact, many polymer suspensions, which containing colloidal particles, have already exhibited nonlinear viscoelastic behavior and been studied for both academic interests and industrial applications. The nonlinear viscoelastic behavior that has been studied includes shear thinning<sup>3–7</sup> and thixotropy,<sup>8–11</sup> which are all related to the grow-up and break-up of particulate aggregate.

It is well known that, with hard particles in colloidal scale, especially when there is at least one dimension of particle, which is smaller than 100 nm, the magnitude of the interparticle force will have a notable effect on the suspension structure and then, the rheological behavior.<sup>12</sup> In fact, the rheological behavior of concentrated suspensions can be affected by a number of factors, such as particle volume fraction, particle size, size distribution, and particle shape.<sup>13,12</sup> In this paper, the effects of filler particle size and concentration on rheological behavior of silicone sealants were investigated with emphasis on shear-thinning behavior and thixotropic property, which are very important for the practical application of silicone sealant.

## EXPERIMENTAL

### Materials and sample preparation

Nano-CaCO<sub>3</sub> and micron-CaCO<sub>3</sub> were supplied by Shanghai Yaohua Nano-Tech Ltd., China. HO-PDMS

Correspondence to: Y. Zhang (yong\_zhang@sjtu.edu.cn).

**TABLE I**  
Particle Parameters of Nano-CaCO<sub>3</sub> and Micron-CaCO<sub>3</sub>

Parameter	Nano-CaCO <sub>3</sub>	Micron-CaCO <sub>3</sub>
Particle shape	Cubic	Cubic
Particle size	50~100nm	1.5~2.1 $\mu$ m
Surface treatment	fatty acid	fatty acid

was provided by Shanghai Resin Factory, China. The detailed parameters of CaCO<sub>3</sub> are shown in Table I.

According to the recipe in Table II, CaCO<sub>3</sub> and HO-PDMS were mixed in a Z-style kneader at 30 rpm for 2 h under a reduced pressure lower than 0.01 MPa. The mixing temperature was kept at 120°C. The resultant compounds were used for rheological measurements.

### Rheological measurements

Dynamic modulus and steady-state shear measurements were performed using an advanced rheometric expansion system (ARES) with a parallel geometry (plate diameter, 40 mm; gap, 1 mm) produced by Rheometrics Scientific, USA. The dynamic measurements were performed in the frequency range from 0.1 to 100 rad s<sup>-1</sup>, whereas the steady-state shear measurements were carried out in the shear rate range from 0.1 to 100 s<sup>-1</sup>. The temperature of the sample chamber was kept at 25.0  $\pm$  0.2°C.

## RESULTS AND DISCUSSION

### Effect of filler particle size on rheological properties of suspensions

#### Dynamic measurement analysis

Figure 1 shows double logarithmic plots of storage modulus  $G'$  and loss modulus  $G''$  as functions of angular frequency  $\omega$  for HO-PDMS suspensions filled with 50.0 wt % nano-CaCO<sub>3</sub> and micron-CaCO<sub>3</sub>, respectively. In comparison with micron-CaCO<sub>3</sub>, nano-CaCO<sub>3</sub> affords the suspensions higher  $G'$  and  $G''$  values in the whole frequency range. With increasing

**TABLE II**  
Recipes of CaCO<sub>3</sub>/HO-PDMS Suspensions

Filler	Mass ratio of filler to HO-PDMS (wt/wt)	Weight fraction of filler (wt %)	Volume fraction of filler (vol %)
Nano-CaCO <sub>3</sub>	0/100	0	0
	20/100	16.7	6.8
	50/100	33.3	15.4
	100/100	50.0	26.7
Micron-CaCO <sub>3</sub>	100/100	50.0	26.1

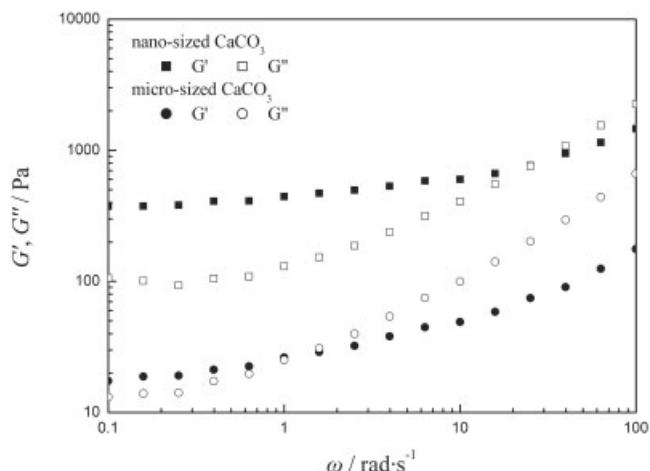


**Figure 1** Double logarithmic plots of  $G'$  and  $G''$  as a function of  $\omega$  for HO-PDMS suspensions filled with nano-CaCO<sub>3</sub> and micron-CaCO<sub>3</sub>, respectively.

angular frequency,  $G''$  increases more remarkably than  $G'$ . As a result, there is an intersection between  $G'$  and  $G''$  for every suspension. When the angular frequency is less than the frequency at the intersection,  $G'$  is higher than  $G''$ , indicating the suspension mainly exhibited elasticity in low frequency region. In the range of high frequency, the suspensions are much viscous. It can be seen that the suspension filled with nano-CaCO<sub>3</sub> exhibits bigger frequency region on the left of the intersection than that with micron-CaCO<sub>3</sub>, indicating nano-CaCO<sub>3</sub> can afford suspension more remarkable elasticity than micron-CaCO<sub>3</sub>.

#### Shear thinning

Shear thinning behavior is a kind of nonlinear viscoelastic behavior. As one of the main characteristics of pseudoplastic fluids, shear thinning behavior is also an important property for silicone sealant and has been studied for various suspensions.<sup>6,14,15</sup> High zero shear viscosity provides silicone sealant with good resistance to deformation, which is necessary for keeping the shape after using in practice. Low shear viscosity at relatively high shear rate can afford silicone sealants good extrusion processibility.

In Figure 2, steady-state viscosity  $\eta$  varies as a function of shear rate  $\dot{\gamma}$  for HO-PDMS suspensions filled with 50.0 wt % nano-CaCO<sub>3</sub> and micron-CaCO<sub>3</sub>, respectively. It can be seen that micron-CaCO<sub>3</sub> filled suspension does not exhibit obvious shear thinning behavior, indicating 50.0 wt % micron-CaCO<sub>3</sub> cannot provide the suspension with good resistance to deformation. In comparison with micron-CaCO<sub>3</sub>, nano-CaCO<sub>3</sub> afforded the suspension higher  $\eta$  value at low shear rate. With increasing shear rate,  $\eta$  value of nano-CaCO<sub>3</sub> filled suspension decreases rapidly, resulting in remarkable shear thinning behavior. It indicates

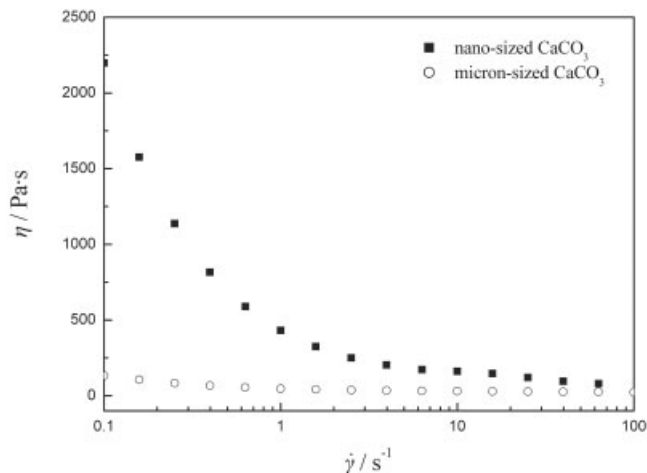


**Figure 2** Plots of  $\eta$  as a function of  $\dot{\gamma}$  for HO-PDMS suspensions filled with 50 wt % nano-CaCO<sub>3</sub> and micron-CaCO<sub>3</sub>, respectively.

50.0 wt % of nano-CaCO<sub>3</sub> is enough to keep a silicone sealant in original shape when a low stress is applied to the silicone sealant. If an intended stress is applied and high enough, an expected extrusion of silicone sealant from package can also be easily achieved. Similar shear thinning behavior has been found in various systems and usually considered to be associated with the break-up of aggregates in a shear field.<sup>7</sup>

To further investigate the effect of shear rate on rheological properties of CaCO<sub>3</sub>/HO-PDMS suspensions, the measured shear stress is fitted to the Casson model, which is one of the most widely used empirical models in previous studies. In fact, many models have been developed to describe the steady-state shear measurement,<sup>16,17</sup> which favor to understand the rheological properties of suspensions. Several models have been used for non-Newtonian systems, such as Casson model, Bingham model, and Krieger-Dougherty model, which have been successfully used to explain, characterize, and predict the flow behavior for various systems.<sup>17-19</sup> The Casson model is described as follows:

$$\tau^{1/2} = \tau_0^{1/2} + \eta_\infty^{1/2} \dot{\gamma}^{1/2} \quad (1)$$

where  $\tau$  is the shear stress,  $\tau_0$  is the yield stress,  $\eta_\infty$  is the suspension viscosity at infinite shear rate, and  $\dot{\gamma}$  is the shear rate.

Figure 3 shows the relationship between the shear stress  $\tau$  and shear rate  $\dot{\gamma}$  for suspensions filled with 50.0 wt % nano-CaCO<sub>3</sub> and micron-CaCO<sub>3</sub>, respectively. A linear relationship between the square root of shear stress and the square root of shear rate can be seen in Figure 3 for the two suspensions, indicating the Casson model is effective to describe the shear rate dependence of shear stress for CaCO<sub>3</sub>/PDMS suspensions.

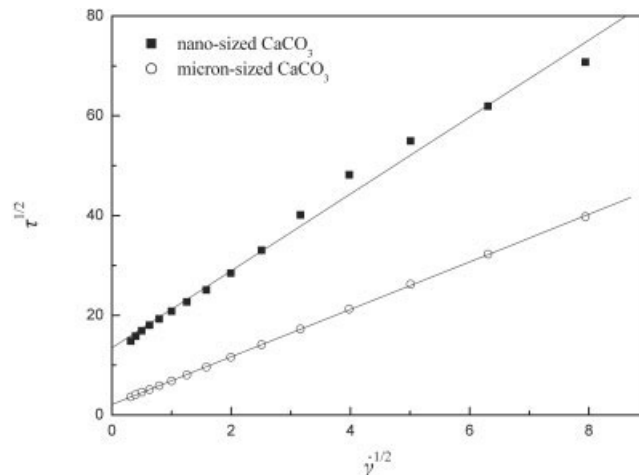


**Figure 3** Plots of  $\tau^{1/2}$  as a function of  $\dot{\gamma}^{1/2}$  for HO-PDMS suspensions filled with 50 wt % nano-CaCO<sub>3</sub> and micron-CaCO<sub>3</sub>, respectively.

An increase in particle volume fraction can increase the viscosity of suspensions and give rise to the yield stress.<sup>13</sup> A high yield stress implies a strong filler network structure existed in a suspension. As a result, high shear stress is needed to break up the filler network structure for practical application, and then, the flow of the suspension can be achieved.

$\eta_\infty$  and  $\tau_0$  are obtained from the slope and intercept of fitted linear regression lines in Figure 3, and listed in Table III. The yield stress of the nano-CaCO<sub>3</sub> filled suspension is much higher than that of the micron-CaCO<sub>3</sub> filled suspension, indicating 50.0 wt % nano-CaCO<sub>3</sub> can establish filler network in suspension, but 50.0 wt % micron-CaCO<sub>3</sub> cannot. This result is reasonable for the interparticle distances are reduced as filler particle size decreases. As a result, the interactions among filler particles increases, and then, more aggregates structure can be formed in suspension.

### Thixotropy

Thixotropy is also an important kind of nonlinear viscoelastic behavior. The term "thixotropy" was originally proposed to describe a rheological phenomenon defined as a reversible decrease in viscosity with shear time when a fluid flowed at constant shear rate. In fact, it is also a kind of shear thinning behavior. Different from general shear thinning behavior, the

**TABLE III**  
 $\tau_0$  and  $\eta_\infty$  Values of Suspensions Filled with 50.0 wt % of Nano-CaCO<sub>3</sub> and Micron-CaCO<sub>3</sub>

Filler	$\tau_0$ (Pa)	$\eta_\infty$ (Pa s)
Nano-sized CaCO <sub>3</sub>	182	59.4
Micron-sized CaCO <sub>3</sub>	4.6	22.7

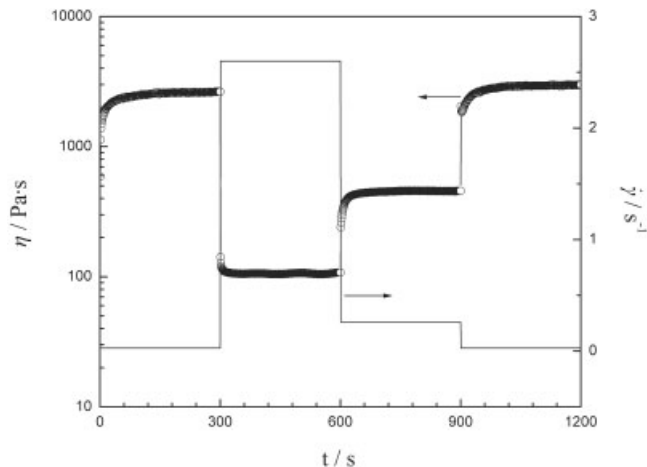


**Figure 4** Shear time dependence of viscosity for suspensions composed of HO-PDMS and 26.7 vol % nano- $\text{CaCO}_3$  in stepwise change of shear rate.

viscosity in thixotropic test was a function of shear time. If a shear time dependence of viscosity is exhibited when applied to a stepwise change of shear rate, the suspension is considered to have thixotropic property.<sup>20</sup>

Figure 4 shows the time dependence of viscosity of the HO-PDMS suspension filled with 50.0 wt % nano- $\text{CaCO}_3$  for stepwise change of shear rate. It can be seen that after stepwise enhancing or reducing the shear rate, the measured viscosity of nano- $\text{CaCO}_3$ /HO-PDMS suspension is always dependent on shear time and achieves steady-state viscosity value gradually. When the shear rate is stepwise changed from 0.026 to  $2.6 \text{ s}^{-1}$ , the viscosity decreases with time, indicating the dependence of the break-up of filler network structure on shear time. When the shear rate was stepwise changed to a low value, such as from 2.6 to  $0.26 \text{ s}^{-1}$ , the viscosity increased with the shear time, indicating the dependence of the grow-up of filler network structure on shear time.

The degree of thixotropy can be determined quantitatively by using the thixotropic loop method.<sup>21</sup> The curves of shear stress versus shear rate, which are increased from zero to a set value and then decreased to zero again, built up a characteristic thixotropic loop. The area of the thixotropic loop can be calculated by integrating the area of ascending and descending shear rate curves, respectively, and then subtracting them to obtain the area value.

The thixotropic loops of suspensions filled with 50.0 wt % nano- $\text{CaCO}_3$  and 50.0 wt % micron- $\text{CaCO}_3$  are shown in Figure 5. It is found that the thixotropic loop of nano- $\text{CaCO}_3$  filled suspension is located above that of micron- $\text{CaCO}_3$  filled suspension. Furthermore, the thixotropic loop area of the nano- $\text{CaCO}_3$  filled suspension is much larger than that of micron- $\text{CaCO}_3$  filled suspension, indicating nano- $\text{CaCO}_3$  favors the buildup of filler network structure in suspension.

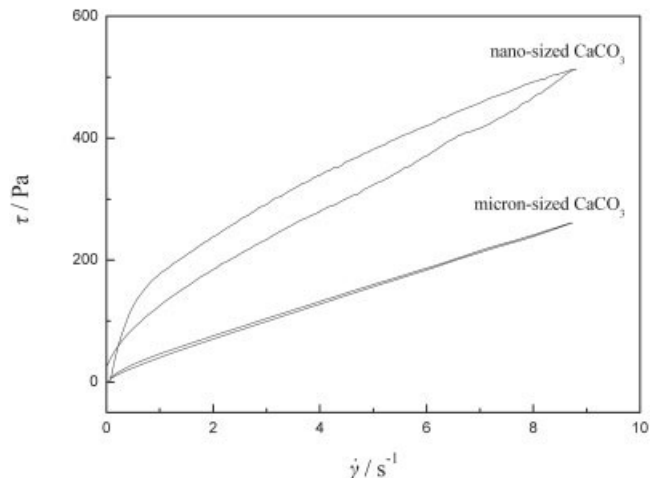


**Figure 5** Thixotropic loops of HO-PDMS suspensions filled with 50 wt % nano- $\text{CaCO}_3$  and micron- $\text{CaCO}_3$ , respectively.

### Effect of nano- $\text{CaCO}_3$ content on rheological properties of suspensions

#### Dynamic measurement analysis

Figure 6 shows double logarithmic plots of storage modulus  $G'$  and loss modulus  $G''$  as functions of angular frequency  $\omega$  for suspensions composed of HO-PDMS and various content of nano- $\text{CaCO}_3$ . Compared with the suspensions containing 15.4 and 26.7 vol % nano- $\text{CaCO}_3$ , the suspension containing 6.8 vol % nano- $\text{CaCO}_3$  exhibits the lowest  $G'$  and  $G''$  values in the whole frequency range. Moreover, its  $G''$  value is always larger than the corresponding  $G'$  value in the whole testing range, indicating the suspension containing 6.8 vol % nano- $\text{CaCO}_3$  mainly exhibit viscosity. With increasing nano- $\text{CaCO}_3$  content, the  $G'$  and  $G''$  values increase simultaneously, and  $G'$  increases

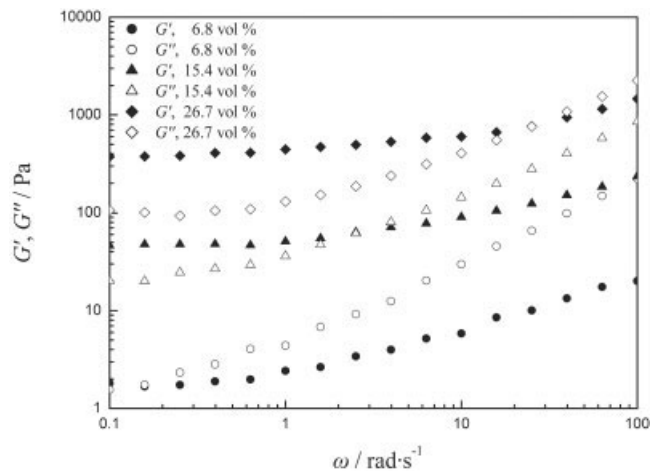


**Figure 6** Double logarithmic plots of  $G'$  and  $G''$  as a function of  $\omega$  for suspensions composed of HO-PDMS and various content of nano- $\text{CaCO}_3$ .

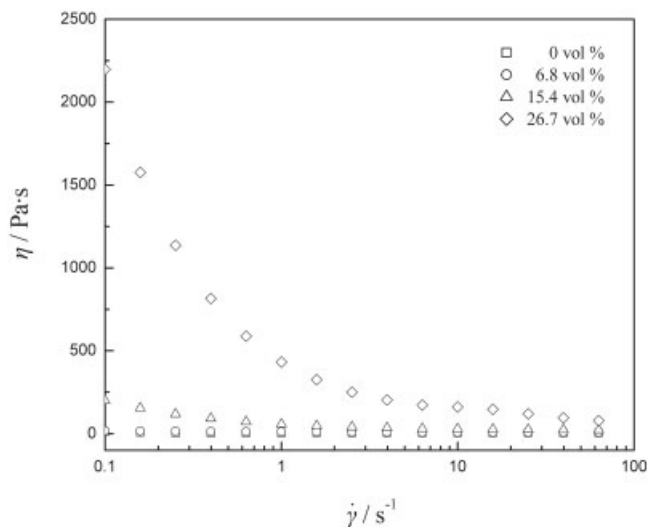


**Figure 7** Plots of  $\eta$  as a function of  $\dot{\gamma}$  for suspensions composed of HO-PDMS and 0, 6.8, 15.4, and 26.7 vol % nano-CaCO<sub>3</sub>.

more remarkably than  $G''$ . High nano-CaCO<sub>3</sub> content leads to a shift of the intersections of  $G'$  and  $G''$  from low frequency region to high one. As a result, the suspensions become more elastic and transformed from a mainly viscous material to a mainly elastic material.

#### Shear thinning

In Figure 7, steady-state viscosity  $\eta$  is shown as a function of shear rate  $\dot{\gamma}$  for nano-CaCO<sub>3</sub>/HO-PDMS suspensions. It is found that  $\eta$  increases remarkably with the increase in filler content at a very low shear rate of 0.016 s<sup>-1</sup>. As the shear rate is increased,  $\eta$  values of various suspensions filled with different content of nano-CaCO<sub>3</sub> approach to each other, though the suspensions with high filler content still have high viscosity. Consequently, the suspensions with high filler content show more obvious shear thinning behavior, indicating high content of nano-CaCO<sub>3</sub> is needed for silicone sealant to keep its shape when applied to a small stress.

Figure 8 shows the relationship between the shear stress  $\tau$  and the shear rate  $\dot{\gamma}$  of suspensions with various content of nano-CaCO<sub>3</sub>. A linear relationship between the square root of shear stress and the square root of shear rate can also be seen, indicating the Casson model is effective to describe the shear rate dependence of shear stress for HO-PDMS suspensions filled with various content of nano-CaCO<sub>3</sub>.

$\eta_{\infty}$  and  $\tau_0$  are obtained from the slope and intercept of fitted linear regression lines in Figure 8, and listed in Table IV. It is seen that the yield stress increases with increasing nano-CaCO<sub>3</sub> content. This result is reasonable, because the interparticle distances are re-

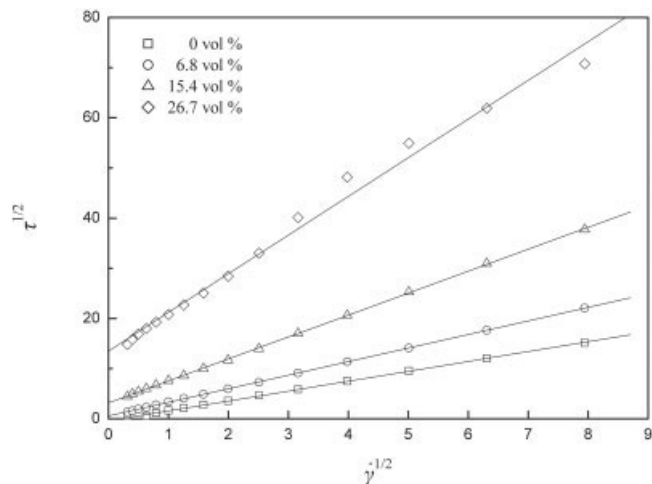


**Figure 8** Plots of  $\tau^{1/2}$  as a function of  $\dot{\gamma}^{1/2}$  for suspensions composed of HO-PDMS and 0, 6.8, 15.4, and 26.7 vol % nano-CaCO<sub>3</sub>.

duced with the increase in nano-CaCO<sub>3</sub> content, which improves the interactions among filler particles and causes more aggregate structure to form in suspensions. The existence of yield stress suggests filler network structure is formed in suspensions with high filler content. As shown in Table IV, the measured viscosity at infinite shear rate ( $\eta_{\infty}$ ) increases with filler content, which is consistent with the result at high shear rate in Figure 7.

#### Thixotropy

The thixotropic loops of silicone sealants filled with various content of nano-CaCO<sub>3</sub> are shown in Figure 9. The thixotropic loops gradually shift to higher shear stress region as the filler content increases. At the same time, the area of thixotropic loop becomes larger. Furthermore, the suspensions exhibit increasing pseudo-plastic properties with increasing filler content. As shown in Table V, the area value of thixotropic loop increases with increasing nano-CaCO<sub>3</sub> content, indicating high content of nano-CaCO<sub>3</sub> favors the buildup of filler network structure in nano-CaCO<sub>3</sub>/HO-PDMS suspensions.

**TABLE IV**  
 $\tau_0$  and  $\eta_{\infty}$  Values of Suspensions with Various Contents of Nano-CaCO<sub>3</sub>

	CaCO <sub>3</sub> content (vol %)			
	0	6.8	15.4	26.7
$\tau_0$ (Pa)	0 <sup>a</sup>	0.35	10.1	182
$\eta_{\infty}$ (Pa s)	3.88	7.29	19.1	59.4

<sup>a</sup> $\tau_0$  value of pure HO-PDMS calculated from Figure 9 is actually a small negative.

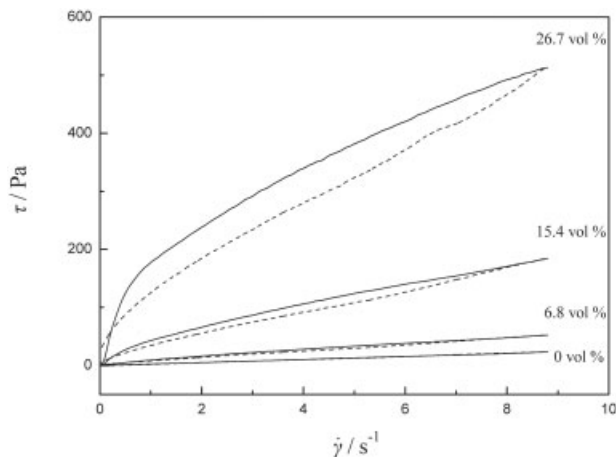


**Figure 9** Thixotropic loops of suspensions composed of HO-PDMS and various contents of nano-CaCO<sub>3</sub>.

#### Overshoot phenomenon

As a kind of typical rheological behavior, overshoot has been frequently observed in suspension studies.<sup>22</sup> It is usually associated with the response of suspension structure to the applied shear stress. When the change of suspension structure could not keep up with the strain induced by shear stress, such overshoot behavior would be observed.

The shear stress  $\tau$  of 26.7 vol % nano-CaCO<sub>3</sub> suspensions as a function of shear time at various shear rates is shown in Figure 10. At low shear rate of 0.05 s<sup>-1</sup>, the shear stress increases gradually to the steady-state viscosity with time. However, at a relative high shear rate such as 0.51 s<sup>-1</sup>, the shear stress increases rapidly to the maximum value at first and then decreases gradually to a steady-state value. This phenomenon is so-called overshoot. As shown in Figure 10, the overshoot of shear stress becomes more pronounced with increasing shear rate. It should be attributed to the slower breakup of filler network structure corresponding to the strain induced by relatively high shear rate. For the suspensions with low nano-CaCO<sub>3</sub> content, such as 6.8 and 15.4 vol %, a similar initial overshoot phenomenon has also been observed, as shown in Figure 11. The difference is that the initial overshoot phenomenon becomes unobvious with the decrease of filler content at the same shear rate. For

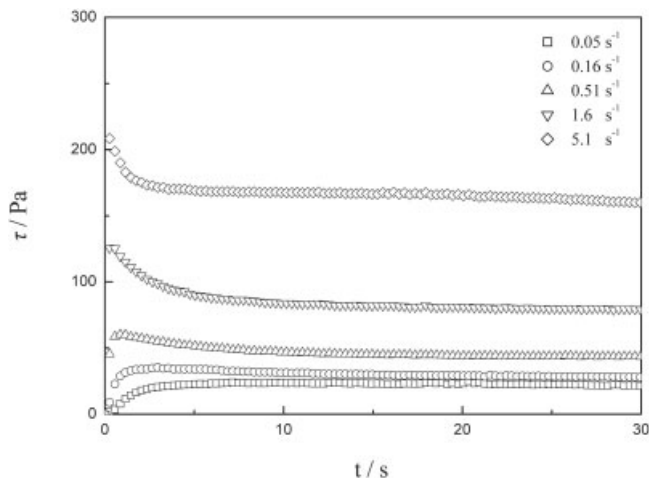


**Figure 10** Plots of shear stress as a function of time for 26.7 vol % nano-CaCO<sub>3</sub> suspension at various shear rates.

pure HO-PDMS, a similar overshoot phenomenon has not been observed evidently, indicating HO-PDMS chains could completely follow the strain immediately in our test.

#### CONCLUSIONS

In comparison with micron-CaCO<sub>3</sub>, nano-CaCO<sub>3</sub> filled suspension exhibits more typical nonlinear viscoelastic behavior such as shear thinning and thixotropy, which could be explained from the break-up and grow-up of filler aggregates. This indicates that filler particle size is an important factor for CaCO<sub>3</sub> if could provide suspension with excellent rheological properties. The Casson model can be used to well fit with the measured shear stresses, indicating its efficiency for describing the shear rate dependence of shear stress

**TABLE V**

**Thixotropic Loop Areas of Various Nano-CaCO<sub>3</sub>/HO-PDMS Suspensions**

nano-CaCO <sub>3</sub> content (vol %)	Thixotropic loop area (Pa s <sup>-1</sup> )
0	2.6
6.8	20.1
15.4	95.3
26.7	431

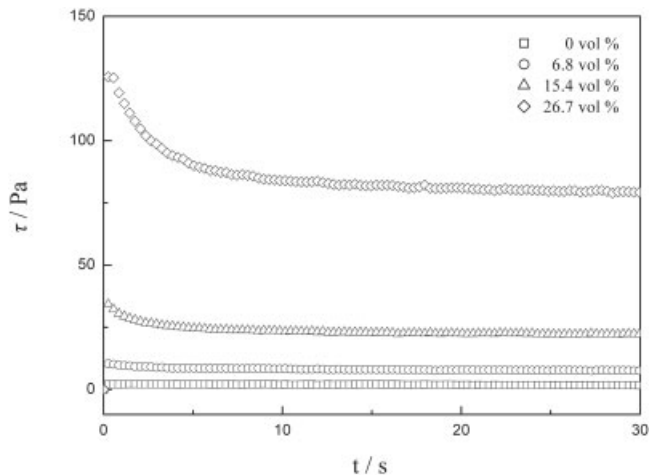


**Figure 11** Plots of shear stress as a function of shear time for nano-CaCO<sub>3</sub>/HO-PDMS suspensions with different filler content at shear rate of 1.6 s<sup>-1</sup>.

for the HO-PDMS/ $\text{CaCO}_3$  suspensions. The existence of yield stress indicates the formation of filler network structure in nano- $\text{CaCO}_3$  filled suspensions with high filler content. The thixotropic loop results indicate that nano- $\text{CaCO}_3$  favors the buildup of filler network structure in nano- $\text{CaCO}_3$ /HO-PDMS suspension. Moreover, high nano- $\text{CaCO}_3$  content favors the establishment of filler network structure in nano- $\text{CaCO}_3$  filled suspensions. Shear thinning and thixotropic phenomena become more remarkable with increasing nano- $\text{CaCO}_3$  content. An overshoot phenomenon can be observed in the nano- $\text{CaCO}_3$ /HO-PDMS suspensions, which should be attributed to the delayed response of suspension structure to applied shear stress.

### References

1. Cochrane, H.; Lin, C. S. *Rubber World, Rubber/Automotive Division of Hartman Communications*: New York, 1985; p 29.
2. Bates, L. P.; Harrison, D. L. In *Adhesives, Sealants and Encapsulants Conference*; London, 1985; Vol. 1, p 131.
3. Andrew, D.; Jones, R.; Leary, B.; Boger, D. V. *J Colloid Interface Sci* 1991, 147, 479.
4. Zhang, L. M.; Jahns, C.; Hsiao, B. S.; Chu, B. *J Colloid Interface Sci* 2003, 266, 339.
5. Wagener, R.; Reisinger, T. *J. G. Polymer* 2003, 44, 7513.
6. Otsubo, Y. *Langmuir* 1994, 10, 1018.
7. Shirono, H.; Amano, Y.; Kawaguchi, M.; Kato, T. *J Colloid Interface Sci* 2001, 239, 555.
8. Hou, W. G.; Sun, D. J.; Han, S. H.; Zhang, C. G.; Wang, G. T. *Colloid Polym Sci* 1998, 276, 274.
9. Li, S. P.; Hou, W. G.; Sun, D. J.; Guo, P. Z.; Jia, C. X. *Langmuir* 2003, 19, 3172.
10. Bournonville, B.; Nzihou, A. *Powder Technol* 2002, 128, 148.
11. Lemke, T.; Bagusat, F.; Köhnke, K.; Husemann, K.; Mögel, H. *J. Colloid Surf A* 1999, 150, 283.
12. Olhero, S. M.; Ferreira, J. M. F. *Powder Technol* 2004, 139, 69.
13. Tseng, W. J.; Lin, K. C. *Mater Sci Eng A* 2003, 355, 186.
14. Cai, J. F.; Salovey, R. *J Polym Sci Part B: Polym Phys* 1999, 37, 815.
15. Barrie, C. L.; Griffiths, P. C.; Abbott, R. J.; Grillo, I.; Kudryashov, E.; Smyth, C. *J Colloid Interface Sci* 2004, 272, 210.
16. Roberts, G. P.; Barnes, H. A.; Carew, P. *Chem Eng Sci* 2001, 56, 5617.
17. Kugge, C.; Daicic, J. *J Colloid Interface Sci* 2004, 271, 241.
18. Hackley, V. A. *J Am Ceram Soc* 1998, 81, 2421.
19. Liu, X. J.; Huang, L. P.; Sun, X. W.; Xu, X.; Fu, X. R. *J Mater Sci* 2001, 36, 3379.
20. Howard, A. B. *J Non-Newt Fluid Mech* 1997, 70, 1.
21. Narayan, R.; Raju, K. V. S. N. *J Appl Polym Sci* 2000, 77, 1029.
22. Kosinski, L. E.; Caruthers, J. M. *J Appl Polym Sci* 1986, 32, 3393.